Original Article

JCBFM

Journal of Cerebral Blood Flow & Metabolism
2016, Vol. 36(12) 2177–2193

DOI: 10.1177/0271678X15615535
jcbfm.sagepub.com
SAGE

The role of the mesolimbic dopamine system in the formation of blood-oxygen-level dependent responses in the medial prefrontal/anterior cingulate cortex during high-frequency stimulation of the rat perforant pathway

Cornelia Helbing[1], Marta Brocka[2], Thomas Scherf[3], Michael T Lippert[2] and Frank Angenstein[1,3]

Abstract

Several human functional magnetic resonance imaging studies point to an activation of the mesolimbic dopamine system during reward, addiction and learning. We previously found activation of the mesolimbic system in response to continuous but not to discontinuous perforant pathway stimulation in an experimental model that we now used to investigate the role of dopamine release for the formation of functional magnetic resonance imaging responses. The two stimulation protocols elicited blood-oxygen-level dependent responses in the medial prefrontal/anterior cingulate cortex and nucleus accumbens. Inhibition of dopamine $D_{1/5}$ receptors abolished the formation of functional magnetic resonance imaging responses in the medial prefrontal/anterior cingulate cortex during continuous but not during discontinuous pulse stimulations, i.e. only when the mesolimbic system was activated. Direct electrical or optogenetic stimulation of the ventral tegmental area caused strong dopamine release but only electrical stimulation triggered significant blood-oxygen level-dependent responses in the medial prefrontal/anterior cingulate cortex and nucleus accumbens. These functional magnetic resonance imaging responses were not affected by the $D_{1/5}$ receptor antagonist SCH23390 but reduced by the N-methyl-D-aspartate receptor antagonist MK801. Therefore, glutamatergic ventral tegmental area neurons are already sufficient to trigger blood-oxygen-level dependent responses in the medial prefrontal/anterior cingulate cortex and nucleus accumbens. Although dopamine release alone does not affect blood-oxygen-level dependent responses it can act as a switch, permitting the formation of blood-oxygen-level dependent responses.

Keywords

Electrophysiology, fMRI, optogenetics, fast-scan cycling voltammetry, hippocampus, ventral tegmental area

Received 21 April 2015; Revised 17 June 2015; Accepted 14 July 2015

Introduction

The mesolimbic pathways link neurons of the ventral tegmental area (VTA) with regions of the limbic system, i.e. the nucleus accumbens (NAcc), amygdala, hippocampus and the medial prefrontal cortex (mPFC). The major transmitter of the mesolimbic pathway is dopamine, and activation of the mesolimbic system with resultant dopamine release into target regions is considered as a pivotal event for a number of cognitive functions, such as various types of learning, reward-

[1]Special Lab for Non-Invasive Brain Imaging, Leibniz Institute for Neurobiology, Magdeburg, Germany
[2]Department of Systems Physiology, Leibniz Institute for Neurobiology, Magdeburg, Germany
[3]Functional Neuromaging Group, Deutsches Zentrum für Neurodegenerative Erkrankungen (DZNE), Magdeburg, Germany

Corresponding author:
Frank Angenstein, Functional Neuroimaging Group, Deutsches Zentrum für Neurodegenerative Erkrankungen (DZNE), Leipziger Str. 44, Magdeburg, Germany.
Email: frank.angenstein@dzne.de

related processes and pain.[1–5] Electrophysiological recordings can easily monitor dopamine-dependent effects on local signal processing, but how these changes eventually lead to an altered global network activity is hard to address, especially because all potential target regions have to be defined in advance. Functional magnetic resonance imaging (fMRI) visualizes localized changes in neuronal activities in the entire brain, so this imaging method does not require the pre-selection of possible target regions. However, fMRI only indirectly visualizes changes in neuronal activity by measuring activity-dependent effects on local hemodynamic parameters, such as blood flow, blood volume or blood oxygenation level.[6–8] Despite its indirect approach, fMRI has been proven to detect even subtle changes in local signal processing; for example, in the hippocampal (HC) formation.[9,10]

Electrical stimulation of the perforant pathway, a fiber bundle projecting onto the dentate gyrus and hippocampus proper, with continuous high-frequency (100 Hz) pulses, has been recently shown to generate significant blood-oxygen-level dependent (BOLD) responses in the HC formation and in various target regions of the mesolimbic system, i.e. mPFC, NAcc and VTA/substantia nigra (SN) region.[11] The appearance of significant BOLD responses in the VTA/SN region indicates that during this stimulation condition HC efferences activate the mesolimbic system via endogenous neural pathways as also shown previously.[1,12] We therefore suggest that this perforant pathway stimulation protocol can serve as a model in which the mesolimbic system is activated by neuronal connections instead of direct stimulation. This allows investigation of the role of the major mesolimbic transmitter, dopamine, in fMRI signals in a more functional context. Previous work, especially phMRI studies have shown that large dopamine increase (e.g. during amphetamine stimulation) controls relative cerebral blood volume (rCBV), thus fMRI measurements can be used as marker for dopamine release.[13] The actions of dopamine are complex and may directly affect microvasculature through $D_{1/5}$ receptors on microvessels (leading to an increased rCBV), act via astroglial D3 receptor (leading to decreased rCBV) and additional neuronal mechanisms.[13–16]

In contrast to continuous high-frequency pulse stimulations, stimulation of the perforant pathway with discontinuous 100 Hz pulses also generated significant BOLD responses in the mPFC and NAcc, but not in the VTA/SN.[17] Therefore, by modifying the stimulation protocol (continuous vs. discontinuous 100 Hz pulses) the mPFC and NAcc become activated either with or without concurrent VTA/SN activation.

In addition, the mesolimbic dopaminergic system can be directly activated by electrical stimulation of the VTA or more specifically by optogenetic activation of mesolimbic dopaminergic neurons.

Using these electrical and optogenetic stimulations as well as pharmacological interventions we addressed the following question: what is the role of dopamine release in the formation of BOLD responses in target regions of the mesolimbic pathway? That is, to what degree does BOLD-fMRI allow conclusions to be drawn about the activation state of the dopaminergic system?

Materials and methods

Animals were cared for and used according to a protocol approved by the animal experiment committee, and in conformity with the European convention for the protection of vertebrate animals used for experimental purposes and institutional guidelines 86/609/CEE, 24 November 1986. The experiments were approved by the animal care committee of the State of Saxony-Anhalt (No.: 203.h.-42502-2-705IfN, 42502-2-1167IfN) and were performed according to the ARRIVE (Animal Research: Reporting *In Vivo* Experiments) guidelines. Male Wistar-Han rats were housed individually in conditions of constant temperature (20°C) and maintained on a controlled 12:12 h light/dark cycle, with food and tap water available ad libitum.

Surgery and electrode implantation

Nine-week-old male Wistar-Han rats (270–330 g) were deeply anesthetized with Nembutal (40 mg/kg, i.p.) and placed in a stereotactic frame. To stimulate the HC formation a bipolar stimulation electrode (114 µm in diameter, Teflon-coated tungsten wire, A-M Systems) was placed into the perforant pathway (AP: −6.9 mm; ML + 4.1 mm from Bregma; DV 2.3–3.0 mm from dural surface) of the right hemisphere, according to the atlas of Paxinos and Watson.[18] For measuring the electrophysiological response in the hippocampus, a monopolar recording electrode (AP: −2.8 mm, ML: −1.8 mm; DV: 2.9-3.5 mm from Dura) was placed in the granular cell layer of the right dentate gyrus. The correct placement of stimulation and recording electrodes during the implantation was verified by measuring monosynaptic field potentials. Silver wire grounding and reference electrodes were placed on the dura of the left skull and fixed with plastic screws and dental cement. For electrical stimulation of the VTA a bipolar stimulation electrode was implanted in the VTA (coordinates: AP −5.6 mm, ML + 2.3 mm from Bregma, DV 7.8 mm from dural surface angled 10° to the midline). The correct placement of the stimulation electrode during the implantation was verified by application of a short stimulation protocol (burst of 10

pulses with an inter-pulse interval of 10 ms, 300 μA stimulation intensity). A correct placement was assumed when this stimulation in the VTA caused clear whisker movements.

Electrical stimulation and functional MRI (fMRI)

All combined electrophysiology/fMRI measurements were performed on a 4.7 T Bruker Biospec 47/20 animal scanner (free bore of 20 cm) equipped with BGA09 (400 mT/m) gradient system (Bruker BioSpin GmbH, Ettlingen, Germany. A 50 mm Litzcage small animal imaging system (DotyScientific Inc., Columbus, SC, USA) was used for the RF signal reception.

All animals were initially anesthetized with isoflurane (1.5–1.8%; in 50:50 N_2:O_2; v:v) and the anesthesia was switched to deep sedation by application of medetomidine (Dorbene, Pfizer GmbH, bolus: 50 μg/kg s.c. and after 15 min 100 μg/kg per h s.c.) after animals were fixed into the head holder and connected to recording and stimulation electrodes.

All necessary MRI and electrophysiological adjustments for the simultaneous fMRI experiment were set in parallel before the measurement began. Breathing, heart rate and oxygen saturation were monitored throughout the experiment by an MRI-compatible pulse oxymeter (MouseOX^{TM}; Starr Life Sciences Corp., Pittsburgh, PA, USA). Heating was provided from the ventral site. To determine the appropriate stimulation intensity for the fMRI experiment the perforant pathway was first stimulated with single test pulses (pulse duration 0.2 ms) at increasing intensities (i.e. 3 test pulses at 10 s intervals with the following intensities: 100, 200, 300, 400, 500, 600 μA; recordings were made at an interval of 2 min except the 600 μA which was taken after a 4-min interval). According to this input/output curve, the stimulation intensity that elicited 50% of the maximal population spike amplitude was determined for each animal and used for the continuous stimulation protocol (i.e. the stimulation intensity for continuous 100 Hz stimulation was between 200 and 300 μA). The pulse intensity for the discontinuous stimulation protocol was set to 250 and 500 μA, which corresponded to intensities that elicited about 50% and 80–90% of the maximal population spike amplitude. The pulse intensity for the VTA stimulation was set to 300 μA, which did not cause clear stimulus-dependent movements of the head.

The perforant pathway was stimulated with the following two general stimulation protocols: (1) continuous 100 Hz pulses and (2) discontinuous 100 Hz pulses, i.e. 8 bursts of 20 pulses applied one burst per second. One stimulation train lasted 8 s, so during the continuous stimulation protocol 800 pulses and during the discontinuous stimulation protocol 160 identical pulses were applied (Figure 1). The applied stimulation protocol consisted of 10 consecutive stimulation trains, given every minute after the 2 min baseline, except for the stimulation protocol that used a continuous stimulation protocol. Because application of continuous 100 Hz pulses occasionally caused the appearance of long-lasting after-discharges the inter-train interval was set to two minutes and only eight consecutive trains were applied.

To test the role of the dopamine $D_{1,5}$ receptors in the formation of a BOLD response during electrical stimulation separate groups of animals were used. One group received the dopamine $D_{1/5}$ receptor antagonist SCH23390 (0.2 mg/kg, i.p.) and another group the agonist SKF83959 (2.0 mg/kg, i.p.) immediately prior to the combined electrophysiology/fMRI session. Because all necessary fMRI and electrophysiological pre-adjustments required about 30 min the combined fMRI and electrophysiological measurement started 30 min after drug application.

The role of N-methyl-D-aspartate (NMDA) receptor activation in the generated BOLD response was tested in an additional group of animals by application of the NMDA receptor antagonist MK801 (0.5 mg/kg, i.p.). MK801 was also applied immediately before the combined fMRI/electrophysiology session.

The electrophysiological responses during stimulation were recorded with a sample rate of 5000 Hz, filtered between 1 and 5000 Hz by using a differential amplifier EX 4-400 (Science Products, Hofheim, Germany), transformed by an analogue-to-digital interface (power-CED, Cambridge Electronic Design, Cambridge, UK) and stored on a personal computer. No further processing filter was needed, because the minor artifacts of the imaging system were small in comparison with the recorded field potential.

For anatomical images 10 horizontal T_2-weighted spin-echo images were obtained with a *RARE* sequence (rapid acquisition relaxation enhanced[19]) with the following parameters: TR 4000 ms, TE 15 ms, slice thickness 0.8 mm, FOV 37×37 mm, matrix 256×256, RARE factor 8, number of averages four. The total scanning time was 8 min 32 s. Functional MRI (fMRI) was performed with a gradient EPI (echo planar imaging) sequence with the following parameters: TR 2000 ms, TE 24 ms, slice thickness 0.8 mm, FOV 37×37 mm, matrix 92×92, total scanning time per frame 2 s. The geometry used for anatomical images and functional images was identical, except the matrix which was 256×256 for anatomical and 92×92 for functional images. Total scanning time for fMRI depended on the used protocols. Continuous 100 Hz pulse stimulation were applied every 2 min for 8 s, thus total time for eight stimulation trains was 17 min (corresponds to 510 frames). Discontinuous 100 Hz

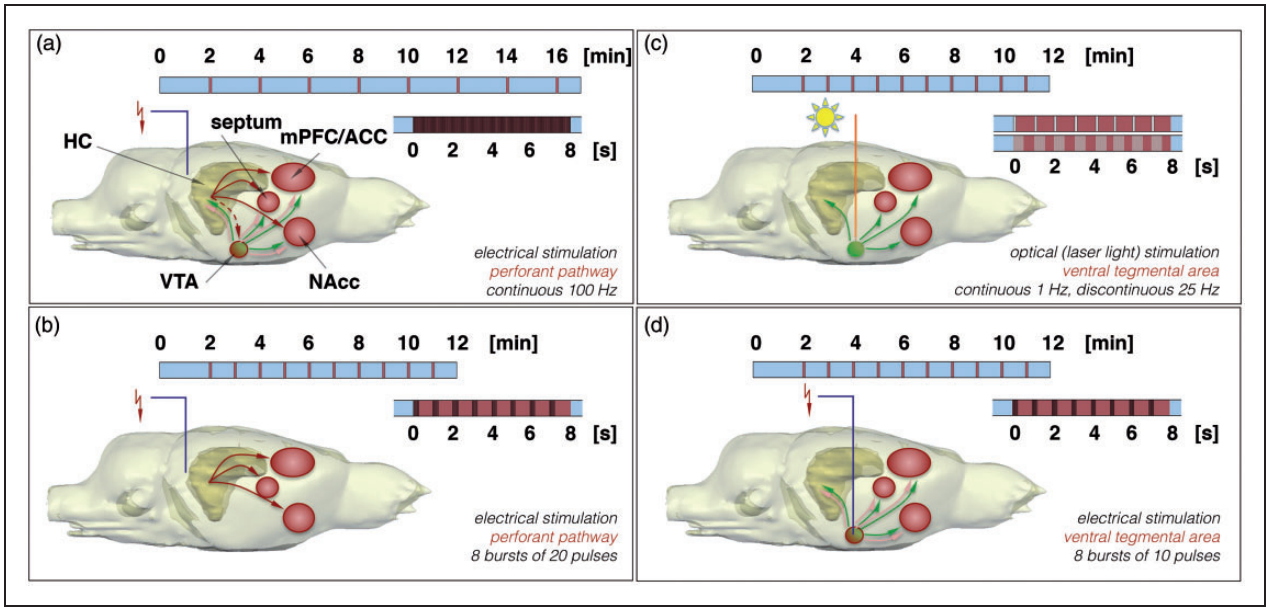

Figure 1. Stimulation protocols and activated pathways. (a) Electrical stimulation of the perforant pathway with continuous 100 Hz pulses for 8 s directly activates the hippocampal formation (HC, indicated by a dark shadow). The HC projects onto the septum, medial prefrontal cortex/anterior cingulate cortex (mPFC/ACC) and nucleus accumbens (NAcc) via glutamatergic fibers (indicated by solid red arrows). In addition, the HC activates the ventral tegmental area/substantia nigra (VTA/SN) region via an indirect pathway (indicated by a dashed red arrow). The VTA in turn projects onto the HC, septum, NAcc and mPFC/ACC via dopaminergic fibers (indicated by green arrows) and via non-dopaminergic fibers (indicated by pink arrows). Therefore, the NAcc, mPFC/ACC and septum receive glutamatergic and dopaminergic inputs. The stimulation protocol is depicted on top as a blue box (see Material and Methods). (b) Electrical stimulation of the perforant pathway with eight bursts of 20 pulses for 8 s with high intensity directly activates the HC (indicated by a dark shadow). Under this condition the HC projects onto the septum, mPFC/ACC and NAcc but not the VTA/SN region. Thus, the NAcc, mPFC/ACC and septum only receive glutamatergic inputs from the HC. (c) Stimulation of the VTA with laser light pulses only activates dopaminergic neurons (indicated by the green color) in this region. These neurons project to the HC, septum, NAcc and mPFC/ACC. The stimulation protocols are depicted on top as a blue box. (d) Electrical stimulation of the VTA directly activates dopaminergic (green) and non-dopaminergic (red) neurons in this region, which in turn project onto target regions of the mesolimbic system. The stimulation protocol is depicted on top as a blue box.

pulse trains were applied every minute after an initial 2 min baseline measurement, thus total time for ten stimulation trains was 11 min (corresponds to 330 frames or 22 min (corresponds to 660 frames).

fMRI data processing and analysis

The functional data were loaded and converted into BrainVoyager data format. A standard sequence of pre-processing steps implemented in the BrainVoyager QX software (Brain Innovation, Maastricht, the Netherlands), such as slice scan time correction, 3D motion correction (trilinear interpolation and reduced data using the first volume as reference) and temporal filtering (high pass GLM-Fourier: three sines/cosines and Gaussian filter; FWHM 3 data points) were applied to each data set. Because the reconstruction of the fMR images resulted in a 128×128 matrix (instead of the 92×92 imaging matrix), a spatial smoothing (Gaussian filter of 1.4 voxel) was added. Functional activation in each individual animal was analyzed by using the correlation of the observed BOLD signal intensity changes in each voxel with a predictor (hemodynamic response function (HRF), generated from the given stimulus protocol (see above); based on this, the appropriate activation map could be generated. To calculate the predictor, the square wave representing stimulus on and off conditions was convolved with a double gamma HRF (onset 0 s, time to response peak 5 s, time to undershoot peak 15 s). To exclude false positive voxels, we only considered those with a significance level p of less than 6.8×10^{-7} ($t_{min} = 5$) for analysis of the size of the activated area, which was thus clearly above the threshold set by calculating the false discovery rate (FDR) with a q-value of 0.05 (which corresponds to a t value greater than three or $p < 0.005$). The BOLD time series depicted for each region represent variations in the BOLD signal intensities of all significantly activated voxels in the corresponding region of interest. When no significantly activated voxels were present (i.e. during receptor inhibition) the BOLD time series

of the region of interest was used for calculation of the response. The BOLD time series shown in all figures are the averages of all the BOLD signal time series measured in all of the individual animals ± standard deviations (SD).

Event-related BOLD responses were calculated by measuring the signal intensities starting six frames before stimulus onset (−12 s until 0 s), during stimulus presentation (between 0 and 8 s, which corresponds to four frames) and the following 15 frames (8 s to 38 s) after the end of the stimulus (Figure 1(a)). To avoid the confounding effect of putative variations in baseline BOLD signal intensities on the calculated BOLD response (i.e. BOLD $\text{signal}_{\text{stimulus}}$/BOLD $\text{signal}_{\text{baseline}}$ × 100%), each BOLD response was related to BOLD signal intensities of the stimulus over the preceding 12 s. The event-related BOLD response for the 2-min intertrain interval protocols were calculated for the following time periods: 10 frames before stimulus onset (−20 s until 0 s), 4 frames during stimulus presentation (0 s to 8 s) and 46 frames after the end of the stimulus (10 s to 100 s) To compare average maximal BOLD responses between conditions, a two-tailed unpaired Student's t-test was performed. To compare the average maximal BOLD responses during consecutive stimulation blocks or between different stimulation conditions during the alternate stimulation protocol, a two-tailed Wilcoxon signed-rank test was performed. Differences were considered significant at a calculated p-value less than 0.05.

To summarize the spatial distribution of significantly activated voxels during a particular stimulation condition, all fMRI data sets were aligned to a 3D standard rat brain using anatomical landmarks. These data sets were then further analyzed with a linear regression analysis (general linear model (GLM) and multi-subject analysis implemented in BrainVoyager QX software). To provide a conservative representation of the main effects, the significance level was set to $t_{min} = 6$ ($p < 7.2 \times 10^{-9}$). All significantly activated voxels were converted into volumes of interest (VOI), from which surface clusters were created and visualized with the BrainVoyager VOI analysis tool.

Optogenetic activation of dopaminergic neurons in the VTA

In optogenetic and combined experiments, wild type or Th::Cre transgenic Long Evans rats were used (Long Evans-Tg(Th-Cre)3.1Deis). For viral transduction of VTA cells with a light-sensitive opsin, an adeno-associated viral vector was injected into the VTA (wild type: AAV2/5-CamKIIα-C1V1(E162T)-p2A-EYFP, Th::Cre: AAV2/5-Ef1a-DIO-hChR2(H134R)-eYFP-WPRE-pA; approximately 2E12 particles/ml, kindly provided by Karl Deisseroth through the UNC Vector Core). The CamKIIα-promoter carried in the virus for wild type animals is primarily expressed in excitatory cells, the majority of which are dopaminergic in the VTA.[20] For transgenic animals, the opsin was directly targeted at tyrosine hydroxylase positive cells via the Cre-loxP system. Two injections of 650 nl virus solution each were performed (AP: −5.6; ML: 0.8 left from Bregma, injection speed was 100 nl/min + 10 min diffusion time per injection) at 7.2 and 7.5 mm depth below the dura.

For laser light delivery, a chronic, custom-made optical fiber was implanted at a depth of 6.9 mm (200 μm diameter, N.A. 0.39). Continuous optogenetic stimulation consisted of 150 ms pulses of green or blue light (wild type: 532 nm custom-made DPSS laser, 2.8 mW at the tip of the fiber implant; Th::Cre: (473 nm custom-made DPSS laser, 3.3 mW) delivered at a rate of 1 Hz for 8 s every 60 s, corresponding to the typical fMRI paradigm used in this study. The radius of opsin activation extended to roughly 400 μm for light intensity of approximately 3 mW/mm^2 and 700 μm for 1 mW/mm^2.[21] Discontinuous optogenetic stimulation consisted of 25 Hz bursts (10 pulses, 10 ms per pulse, 10 mW intensity), also delivered once per second for 8 s.

To confirm behaviorally relevant dopamine release upon illumination, we trained animals to perform intracranial self-stimulation (ICSS). The ICSS paradigm consisted of 10 consecutive sessions of 30 min of daily training. In order to get light stimulation, the rats had to press a nose poke lever. Each press resulted in either a single pulse or a single burst of light (parameters equivalent to fMRI stimulation paradigm). In the continuous stimulation group, one subgroup of rats was trained before fMRI scanning and one subgroup after fMRI scanning to exclude effects from plastic changes owed to the stimulation (n = 5 WT, 1 Th::Cre).

After completion of all experiments, animals were perfused and the brain extracted. Fiber position and virus expression was confirmed histologically (Figure 2). Dopaminergic cells were stained with primary antibody against tyrosine hydroxylase (1:1000 polyclonal rabbit anti-Th, Abcam ab112) and fluorescent secondary anti-rabbit antibody.

Fast-scan cyclic voltammetry

Fast-scan cyclic voltammetry (FSCV) was performed with polymer-encased carbon fiber electrodes (7 μm diameter, ~100 μm length; Toray Carbon Fibers America, Inc., Santa Ana, CA, USA) as an acute procedure. The Ag/AgCl reference electrode was prepared from silver wires (0.5 mm diameter, Sigma-Aldrich, St Louis, MO, USA) chloridized in 0.1 M HCl. The cyclic voltammograms were obtained with a triangular waveform (scan rate: 10 Hz, resting potential: − 0.4 V,

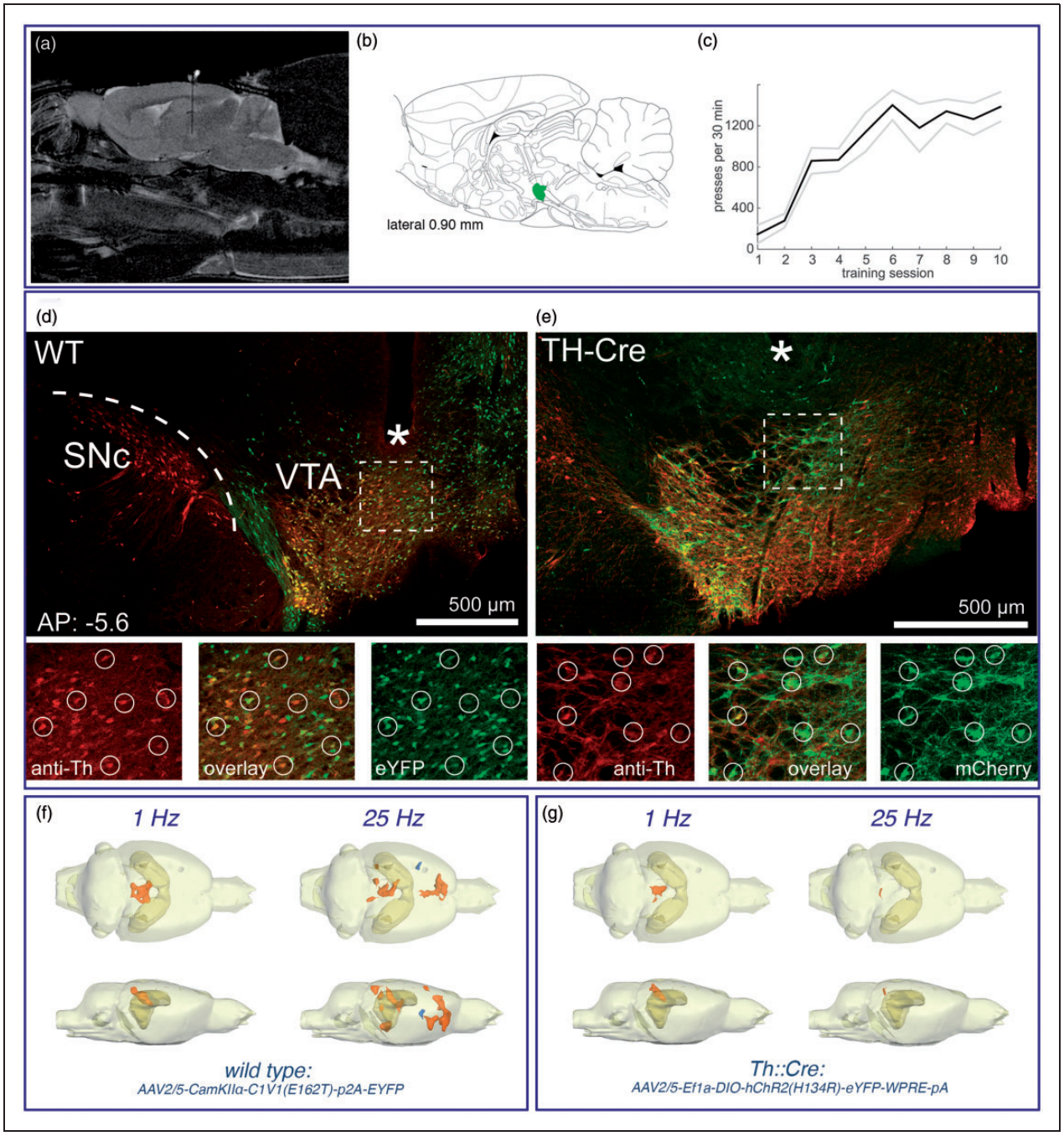

Figure 2. Optogenetic stimulation of dopaminergic neurons in the VTA. (a) An optical fiber was chronically implanted to deliver pulses of laser light to the VTA region. (b) The location of the VTA is indicated by the green color in the schematic brain atlas.[18] (c) To confirm the right position the rats were trained to perform intracranial self-stimulation tasks. (d, e) Histological confirmation of opsin expression and fiber placement. WT: the CamKIIα-promoter led to expression of the green-fluorescent optogenetic construct around the injection site in the VTA. No expression of protein is evident in the dopaminergic cells of the Substantia nigra (SNc). Because of the placement of the fiber tip (*) close to the VTA, light spread is limited to this region and excitatory cells transduced further away from the tip are not excited by green light application. The smaller panels show a magnified view of the region below the fiber tip. A good correspondence between Tyrosine hydroxylase (TH) immunofluorescence (red) and opsin expression (green) is visible (circles), but not all dopaminergic cells have been transduced and some cells express opsin without also showing TH-immunofluorescence. TH-Cre: opsin expression (green) and Th-Immuno stain (red) in the same region as above but in transgenic rats expressing Cre-recombinase under the Th-promoter. Similarly to wild-type rats there is good co-localization of opsin expression and tyrosine-hydroxylase as expected from the Cre-loxP system. (f, g) BOLD response pattern caused by optogenetic activation of the VTA in wild-type rats (f) during 1 Hz ($n = 10$) or 25 Hz ($n = 6$) pulse stimulations and in TH-Cre rats (g) during 1 Hz ($n = 2$) or 25 Hz ($n = 6$) pulse stimulations. The location of the hippocampus is indicated by the dark ocher color. Regions with stimulus-related significantly increased BOLD signal intensities are marked in red and regions with stimulus-related significantly reduced BOLD signal intensities are marked in blue.

switching potential: 1.3 V, 400 V/s, 1000 samples per scan). Waveform generation and data collection were performed with the Invilog Voltammetric System and Software (Acquisition and Stimulation A&S, Invilog Research Ltd, Kuopio, Finland) and analyzed by a FSCV analysis (Invilog Research Ltd, Kuopio, Finland) tool, which integrates FSCV and displays electrochemical measurements on a base station computer. The FSCV carbon fiber electrode was placed in the NAcc (AP: 1.2 mm, ML: 1.5 mm from bregma, DV: 6.6–7.0 mm from the dural surface). The peak oxidation currents for dopamine in each voltammogram (at approximately 0.6 V) were converted into concentration from a post-experiment calibration against fresh solutions of 0.1 to 2 M dopamine.

Statistical evaluation

All values are given as mean ± standard deviation. The statistical analyses were performed with the SPSS software package (19.0). Prior to statistical analysis, data were tested for normality to choose the appropriate test. The error level was set to $\alpha = 0.05$. For statistical comparison of values between the individual experiments, the nonparametric Wilcoxon–Mann–Whitney-test was used ($*p < 0.05$, $**p < 0.01$, $***p < 0.001$), unless stated otherwise.

Results

To study the influence of dopaminergic transmission on the BOLD signals in mPFC/ACC and NAcc two related perforant pathway stimulation protocols were applied: a continuous and a discontinuous 100 Hz pulse protocol.[11,17] Both protocols reliably induce BOLD responses in mPFC/ACC and NAcc, but differ in their ability to generate significant BOLD responses in the VTA/SN region. Only the continuous stimulation protocol triggered significant BOLD responses in the VTA/SN region.

To address the contribution of dopamine for the formation of significant BOLD responses in the mPFC/ACC and NAcc we applied the dopamine $D_{1/5}$ receptor antagonist, SCH23390, or the $D_{1/5}$ receptor agonist SKF83959 before perforant pathway stimulation. In addition, we directly stimulated the VTA either electrically or optogenetically to evoke dopamine release into the mPFC/ACC and NAcc (Figure 1).

Dopamine receptor activation is necessary for the formation of BOLD responses outside the HC formation during continuous perforant path stimulation

As previously observed,[11] repetitive electrical stimulations of the perforant pathway with continuous 100 Hz pulses induced significant BOLD responses in the entire HC formation, in the septum, in the NAcc, mPFC/ACC and in the VTA/SN region ($n = 13$, Figure 3, Table S1). Outside the HC formation stronger BOLD responses were induced after the second stimulation train, and thus repetitive trains were required to elicit maximal BOLD responses. In the hippocampus, the BOLD signal intensities remained elevated after cessation of the first stimulus train. Simultaneously recorded electrophysiological responses in the DG revealed the appearance of heavy neuronal after-discharges after the first stimulation trains.[11] Therefore, these after-discharges are most likely the cause of the sustained BOLD signal increase after the first stimulus train.

The presence of the specific dopamine $D_{1/5}$ receptor antagonist SCH23390 during the stimulation suppressed the formation of significant BOLD responses in the mPFC/ACC and significantly decreased the BOLD responses in the NAcc and septum ($n = 11$, Figure 3, Table S1). It did not, however, modify the BOLD response in the right hippocampus.

Application of the NMDA receptor antagonist MK801 before stimulation resulted in significantly shorter durations of individual BOLD responses in the right hippocampus, which coincided with lesser or even absent after-discharges of granular cells after cessation of the electrical stimulation. Outside the HC formation significantly reduced BOLD responses were observed in the VTA/SN, NAcc and mPFC/ACC ($n = 8$, Figure 3, Table S1). Thus, outside the HC formation the BOLD response critically depended on NMDA receptor-mediated mechanisms.

Continuous perforant pathway stimulation activates the mesolimbic dopamine system

The inhibitory effect of the dopamine receptor antagonist SCH23390 on the BOLD response suggests a crucial involvement of the dopaminergic system in the generation of a BOLD response in regions outside the HC formation. However, this result does not clarify the source of the dopaminergic action, which could be ongoing (baseline) activity or stimulus-induced activity of the mesolimbic system.

A mesolimbic origin of the dopaminergic activity is indicated by the BOLD response pattern of continuous stimulation paradigm. Repetitive stimulation with continuous 100 Hz pulses caused significant BOLD responses in the VTA/SN region that even increased after the second pulse train. Concurrently, the BOLD responses in the mPFC/ACC, NAcc increased in a similar manner (Figure 3). The appearance of significant BOLD responses in the VTA/SN region points to an increased neuronal activity in this region. Because of the cellular heterogeneity of the region, it is unclear

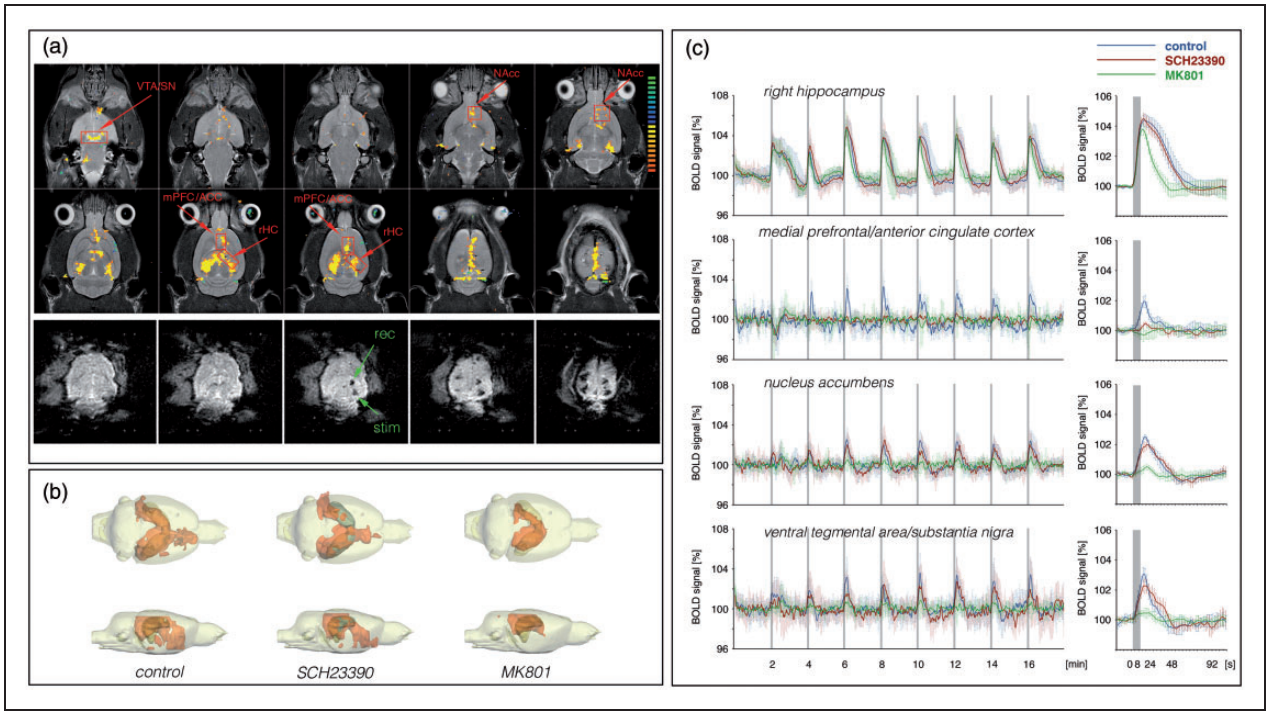

Figure 3. BOLD response pattern during electrical stimulation of the perforant pathway with continuous 100 Hz pulses for 8 s. (a) Spatial distribution of significantly activated voxels in one animal during repetitive stimulations of the perforant pathway. The analyzed regions of interest (ROIs) are indicated by red boxes.
Implanted electrodes causes minor artifact (green arrows, rec = monopolar recording electrode, stim = bipolar stimulation electrode) in the raw EPI data set. (b) Summary of the distribution of significant BOLD responses during repetitive stimulations of the perforant pathway under control conditions (n = 13), in the presence of SCH23390 (n = 11) and MK801 (n = 8). (c) Comparison of the BOLD time series of all significantly activated voxels in the corresponding ROI during the three conditions. The gray boxes indicate the locations of stimulation trains. Averaged BOLD responses of the last six trains are summarized at the right-hand side (green asterisk indicate significant differences between the control and MK801 treated group and blue asterisk indicate significant differences between the control group and SCH2330 treated group).
HC: hippocampal formation, NAcc: nucleus accumbens, mPFC/ACC: medial prefrontal cortex/anterior cingulate cortex, VTA/SN: ventral tegmental area/substantia nigra.

whether the response is causally linked to the activation of dopaminergic or non-dopaminergic cells. To establish a possible relationship between this observed BOLD activation and dopamine release into the NAcc, we performed in vivo FSCV. Electrical stimulation of the perforant pathway with continuous 100 Hz pulses for 8 s caused a detectable release of dopamine into the NAcc (n = 4, Figure 4(a)). Furthermore, consecutive stimulations of the perforant pathway caused consecutive dopamine releases. Therefore, the continuous stimulation paradigm indeed induces dopamine release, which is also not rapidly depleted.

Dopamine release into the mPFC/ACC or NAcc is not sufficient to elicit BOLD responses in mPFC/ACC, NAcc and septum

To further investigate whether the observed BOLD response in the mPFC/ACC, NAcc and septum was the result of an evoked dopamine release into these regions we used an optogenetic approach selectively to activate dopaminergic neurons in the VTA. Laser light application to the VTA transduced with a light sensitive opsin in this region caused a massive dopamine release in the NAcc, as confirmed by in vivo FSCV (n = 6, Figure 4(b)). The appetitive effect of this dopamine release was also evidenced by the strong self-stimulation behavior that was acquired after this optogenetic intervention (Figure 2(c)). However, optogenetic stimulation of dopaminergic cells in the VTA did not induce any significant changes in BOLD signal intensities in the mPFC/ACC, NAcc or in the septum, during either the 1 Hz or the 25 Hz stimulation protocol (n = 6). Significant changes in BOLD signal intensities were only observed in the region of colliculus superior (Figure 4(b)). Therefore, a substantial release of dopamine into target regions of the mesolimbic system is not sufficient to explain extra-HC BOLD responses evoked by the continuous stimulation paradigm.

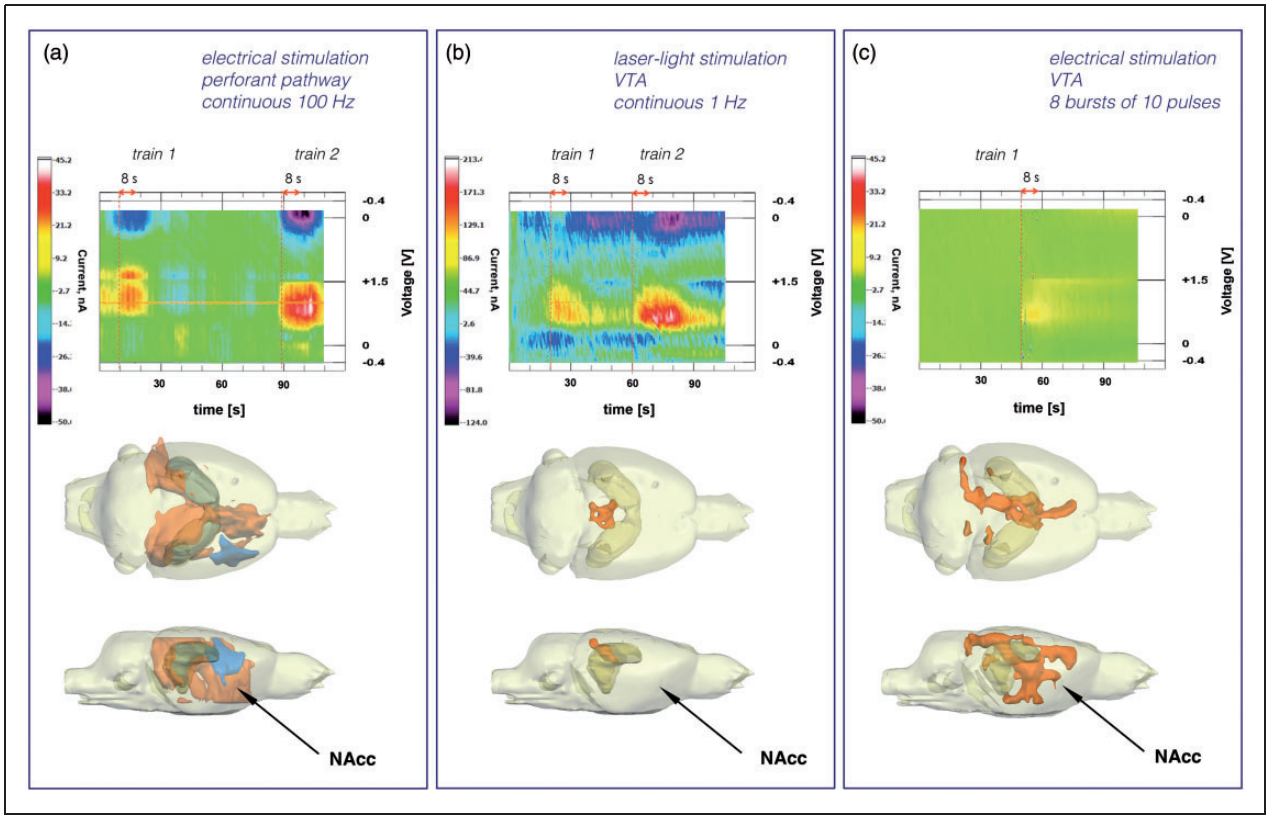

Figure 4. Dopamine release into the nucleus accumbens as detected by in vivo fast-scan cyclic voltammetry. (a) Stimulation of the perforant pathway with continuous 100 Hz pulses for 8 s caused a detectable dopamine release into the NAcc (1.4 ± 0.2 μM). The dopamine release was transient and repeatable during consecutive stimulations (top part). The same stimulation protocol caused the generation of a widespread BOLD response in the rat brain including the NAcc region (lower part, arrow). (b) Laser light stimulation of dopaminergic neurons in the VTA caused a substantial transient dopamine release into the NAcc (4.6 ± 0.6 μM, top part). The dopamine release into the NAcc was not accompanied by significant changes in BOLD signal intensities in the NAcc area (lower part, arrow). Only in the colliculus superior region were significant stimulus-dependent changes in BOLD signal intensities observed. (c) Electrical stimulation of the VTA regions by 10 pulses at 100 Hz repetition rate caused transient dopamine release into the NAcc (3.5 ± 0.4 μM). The same stimulation protocol caused a complex significant BOLD response that included the NAcc region (lower part, arrow).

BOLD responses outside the HC formation induced by discontinuous perforant pathway stimulation are not linked to dopamine $D_{1,5}$ receptors

In a second set of experiments the perforant pathway was stimulated with discontinuous 100 Hz pulses, i.e. with eight bursts of 20 pulses in each train, or with only one-fifth of the pulses used for the continuous stimulation protocol (Figure 1). The stimulation current during the first 10 trains was adjusted to 250 μA and during the following 10 trains to 500 μA. During the first 10 trains significant BOLD responses were induced in the HC formation and weak BOLD responses were induced in the mPFC/ACC, indicating that the stimulation intensity of 250 μA is just above the threshold to elicit significant BOLD responses outside the HC formation. Doubling the stimulation intensity during the following 10 trains resulted in increased BOLD responses in the right HC and mPFC/ACC and the appearance of significant BOLD responses in the NAcc but not in the VTA/SN region ($n = 5$, Figure 5, Table S2). Therefore, this stimulation protocol was not sufficient to cause detectable BOLD responses in the VTA/SN region. Furthermore, the discontinuous stimulation protocol triggered more uniform BOLD responses outside the HC formation, i.e. the first two trains did not generate significantly smaller BOLD responses in the mPFC/ACC or NAcc (Figure 5).

The presence of the dopamine $D_{1/5}$ receptor antagonist SCH23390 during this stimulation protocol did not significantly reduce the BOLD responses in the mPFC/ACC and NAcc ($n = 5$, Figure 5, Table S2). That means that during this stimulation condition a stimulus-induced activation of dopaminergic system is not required for the formation of BOLD responses

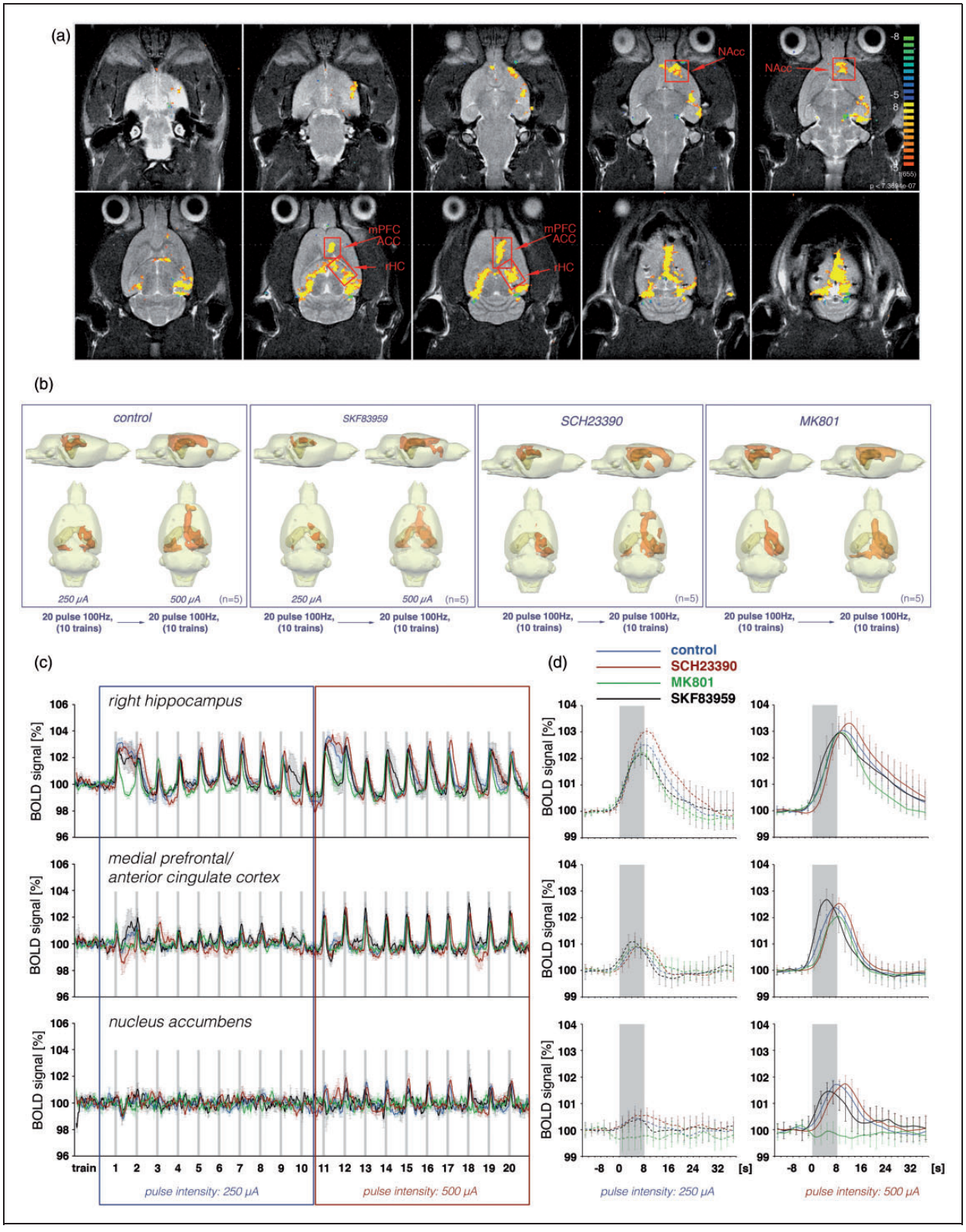

Figure 5. BOLD response pattern during electrical stimulation of the perforant pathway with eight bursts of 20 pulses for 8 s. (a) Spatial distribution of significantly activated voxels in one animal during repetitive stimulations of the perforant pathway. (b) Three-dimensional visualization of significantly activated regions during repetitive stimulations of the perforant pathway with 10 trains of

(Continue)

outside the HC formation. Furthermore, ongoing or baseline activity of the dopaminergic system is not required for the generation of BOLD responses in these regions. To test if under this condition an additional activation of dopamine $D_{1/5}$ receptors affects the BOLD response in these three regions, the same stimulation protocol was applied in the presence of the dopamine receptor agonist SKF83959. Application of SKF83959 before starting the combined electrophysiology-fMRI session did not increase the maximal BOLD responses in the mPFC/ACC, NAcc or septum, either during stimulation with 250 μA or during stimulation with 500 μA (n = 5, Figure 5). Although SKF83959 did not alter the maximal BOLD response, the presence of SKF83959 changed the shape of the HRF, most obviously in the mPFC/ACC. In the mPFC/ACC the time between stimulus onset and reaching the maximum BOLD signal intensity was significantly reduced by more than 2 s (Figure 5, Table S2).

Application of the dopamine agonist SKF83959 before the stimulation protocol continuously affects the dopaminergic system as long as a sufficient concentration of the agonist is present in the vicinity of dopamine receptors; thus this experimental approach does not allow for stimulus-coupled variations in dopaminergic actions. To couple the synaptic dopamine release temporarily with the applied perforant pathway stimulation we used combined electrical and optical stimulation of the perforant pathway and VTA region respectively. Laser light-induced co-activation of the VTA during perforant pathway stimulation did not significantly modify the generated BOLD responses in the mPFC/ACC, NAcc and septum despite a strong dopamine release (n = 5, Figure S1).

Similar to the continuous pulse stimulation experiments, the presence of the NMDA receptor antagonist MK801 also inhibited the formation of significant BOLD responses outside the HC formation during discontinuous 100 Hz pulse stimulations (n = 5, Figure 5(b) to (d)). In contrast to the effect during continuous stimulation, MK801 completely inhibited the BOLD response in the NAcc, whereas in the mPFC/ACC NMDA receptor inhibition only reduced the magnitude of the BOLD response by about 14% (Figure 5(d), Table S2). Thus, during discontinuous perforant pathway stimulation the formation of significant BOLD responses in the NAcc critically depends on the activation of NMDA receptors, whereas in the mPFC/ACC these receptors are less important.

In summary, discontinuous 100 Hz pulse stimulations of the perforant pathway resulted in significant BOLD responses in the HC formation, mPFC/ACC, NAcc and septum. No activity was detected in the VTA/SN region. Under these conditions, neither the activation of postsynaptic $D_{1/5}$ dopamine receptors nor the activation of NMDA receptors is necessary to generate significant BOLD responses in the mPFC/ACC.

Direct electrical stimulation of the VTA causes significant BOLD responses in the mPFC/ACC and NAcc

The results described above show an apparent discrepancy. On the one hand, dopamine release is necessary for the generation of BOLD responses in the mPFC/ACC (i.e. during continuous 100 Hz stimulation). On the other hand, such BOLD responses also occur without any dopamine release and even in a way that is completely insensitive to additional dopamine receptor activation (i.e. during discontinuous 100 Hz stimulation). Furthermore, dopamine release alone is also incapable of reproducing the observed activation patterns. To resolve this discrepancy, we employed electrical VTA stimulation.

One hypothesis is that a complex activation of heterogeneous VTA neurons is required to control the BOLD response in target regions of the VTA. The VTA consists not only of dopaminergic neurons but also of glutamatergic and GABAergic neurons.[22] To test the possibility that only co-activation of different classes of neurons in the VTA enables the generation of a dopamine-dependent BOLD response in the mPFC/ACC, we electrically stimulated the VTA with either 1 Hz pulse trains or discontinuous 100 Hz pulse trains, i.e. 8 bursts of 10 pulses, one burst per s. Electrical stimulation at 1 Hz pulses did not induce any detectable change in BOLD signal within the entire brain. In contrast, electrical stimulation of the VTA with discontinuous 100 Hz pulses resulted in clear BOLD responses in the mPFC/ACC, NAcc and septum (n = 7, Figure 6(a), Table S3). Similarly, 1 Hz stimulation did not result in a detectable dopamine release in the NAcc, whereas

Figure 5. (Continued)
low-intensity pulses (250 μA) and during the subsequent 10 trains with high-intensity pulses (500 μA) during control conditions (n = 5) or in the presence of SKF83959 (n = 5), SCH23390 (n = 5) or MK801 (n = 5). (c) Summary of the BOLD time series in the right hippocampus, medial prefrontal cortex and nucleus accumbens during control condition (blue lines), in the presence of SCH23390 (red lines), MK801 (green lines) or SKF83959 (black lines). (d) The averaged responses to the last eight trains for the two conditions, i.e. during low- and high-intensity pulse intensities, are depicted at the right-hand side.

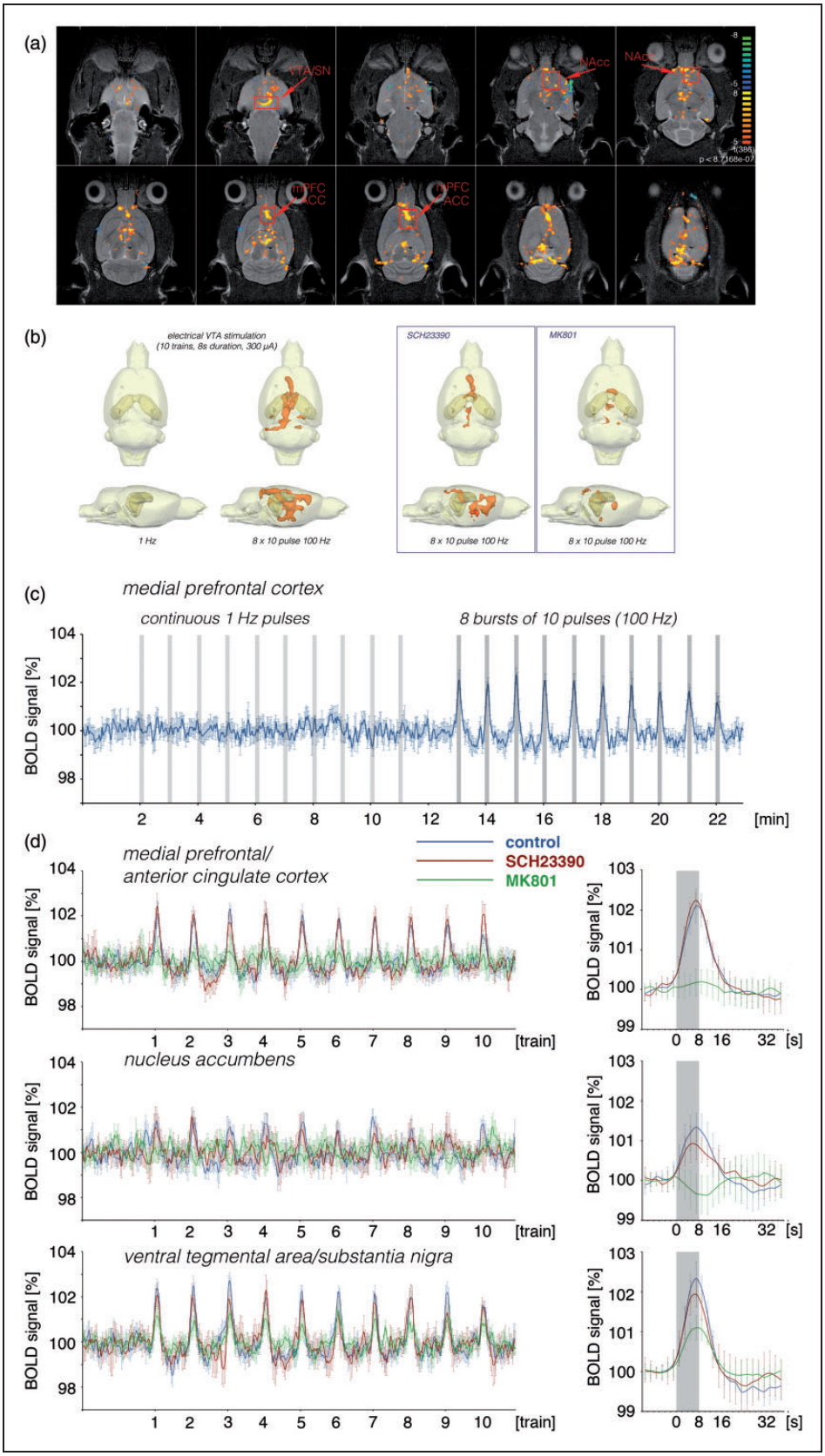

Figure 6. BOLD response pattern during electrical stimulation of the ventral tegmental area with continuous 1 Hz pulses or eight bursts of 10 pulses for 8 s. (a) Spatial distribution of significantly activated voxels during electrical stimulation of the VTA in one animal. (Continue)

discontinuous 100 Hz stimulation did (n = 2, Figure 4). A stimulus-induced BOLD responses was already observed during the first stimulation train and the BOLD responses did not significantly increase after the second train.

Surprisingly, replicating the experiment in the presence of the dopamine $D_{1/5}$ receptor antagonist SCH23390 did not abolish the BOLD responses in the mPFC/ACC and NAcc as we observed during the continuous perforant pathway stimulation protocol.

However, presence of the NMDA receptor antagonist MK801 completely inhibited the formation of significant BOLD responses in the mPFC/ACC and NAcc, indicating that the formation of BOLD responses in these regions during electrical VTA stimulation is mainly controlled by NMDA receptor-mediated mechanisms and not by dopamine $D_{1/5}$ receptor-mediated mechanisms (Figure 6(b), Table S3).

To confirm a possible role of glutamatergic neurons in the VTA for the formation of BOLD responses in the mPFC/ACC and NAcc during electrical stimulation of the VTA we took advantage of the fact that opsins, when expressed under control of the CamKIIα promoter, are also present in non-dopaminergic, excitatory cells, i.e. glutamatergic cells (Figure 2(d)). Optogenetic stimulation of the VTA in these rats also caused significant BOLD responses in the mPFC/ACC and NAcc (n = 6, Figure 2(f)). This result indicates that glutamatergic neurons in the VTA can drive BOLD responses in target regions of the mesolimbic system without requiring concurrent dopamine release.

Discussion

The current study was aimed at investigating how dopaminergic transmission controls the formation of fMRI BOLD responses in two main target regions of the mesolimbic pathway, the mPFC/ACC and NAcc. The main results of the current study are: (1) glutamatergic inputs from HC or VTA neurons are sufficient to generate significant BOLD responses in the mPFC/ACC and NAcc; (2) mesolimbic dopaminergic inputs alone are not sufficient to induce significant BOLD responses in the mPFC/ACC or NAcc; (3) stimulus-induced co-release of dopamine in mPFC/ACC can be required to evoke significant BOLD responses.

Optical vs. electrical stimulation of the VTA

One result of the current study was the unexpected and strong difference in BOLD activation patterns induced by electrical or optogenetic VTA stimulation. Although both kinds of stimulation caused similar dopamine releases, optogenetic activation did not induce the same widespread BOLD activation pattern that electrical stimulation did. This result confirms previous observations that optogenetic and electrical stimulation of an identical structure can cause fundamentally different neuronal activation patterns and highlights the advantage of optogenetic methods in targeting subclasses of neurons.[23]

We found that VTA stimulation-induced BOLD responses did not primarily depend on dopamine release but on glutamatergic transmission. In particular, BOLD responses induced by electrical stimulation of the VTA were not affected by $D_{1/5}$ receptor inhibition but were completely blocked by the NMDA receptor inhibitor MK801. Similarly, specific optogenetic stimulation of VTA dopaminergic neurons in Th::Cre rats did not induce significant BOLD responses in the mPFC/ACC or NAcc during either the 1 Hz or the 25 Hz pulse protocol. In contrast, optogenetic stimulation of dopaminergic and glutamatergic neurons in the VTA of wild-type rats induced detectable BOLD responses in the mPFC/ACC and NAcc, especially during the initial stimulation trains. Histology confirmed that for CamKIIα-driven expression the opsin was expressed in a significant number of Th-negative cells (Figure 2(d)), which are probably glutamatergic.[24] These results also imply that glutamate co-release from dopaminergic neurons[25–28] is insufficient to drive BOLD responses but that co-activation of glutamatergic neurons in the VTA is sufficient.

Although optogenetic stimulation of glutamatergic and dopaminergic VTA neurons causes detectable BOLD responses in the mPFC/ACC and NAcc there are still quantitative and qualitative differences compared with electrical stimulation of the same structure. The reasons may be manifold. The VTA contains not only dopaminergic[22,29,30] and glutamatergic neurons[31–33] but also a number of GABAergic neurons.[22,34,35] Neither Th::Cre-selective or CamKIIα-selective optogenetic stimulation directly affects GABAergic cells in the VTA. Furthermore,

Figure 6. (Continued)
Red boxes mark the regions of interest. (b) Three-dimensional visualization of significantly activated regions during repetitive electrical stimulations of the VTA with continuous 1 Hz pulses or eight bursts of 10 pulses. (c) The corresponding BOLD time series in the mPFC/ACC under control condition revealed that the generation of similar BOLD responses requires more than a continuous 1 Hz-pulse stimulation. (d) Comparison of the BOLD time series in the three regions under control condition (blue lines, n = 7), in the presence of SCH23390 (red lines, n = 7) and MK801 (green lines, n = 7). To visualize the effects of the two antagonists the averaged BOLD responses (train 1–10) are depicted in the right-hand panel.

GABAergic cells cannot be directly responsible for the observed effects, as pharmacological manipulation showed a necessity for glutamatergic activity. They may, however, modulate the evoked activation pattern of glutamatergic cells and through this process affect the generated BOLD response indirectly.

An additional point that has to be considered is that extracellular electrical stimulation induces a complex pattern of excitation and inhibition of neuronal elements and acts differentially on cell bodies and fibers.[36] Most importantly, it not only causes anterograde activation—as the employed optogenetic approach does—but also retrograde activation of regions projecting onto the VTA. It is tempting to speculate that electrical stimulation of the VTA activates a more complex neuronal circuit that eventually controls the BOLD response in the mPFC/ACC through remote glutamatergic action in combination with local dopamine release. It remains for further studies to locate the responsible processes more precisely.

VTA and HC inputs in the mPFC/ACC and NAcc and control by dopamine

Electrical stimulation of the perforant pathway causes an activation of the HC formation, which in turn projects, inter alia, onto the mPFC/ACC and NAcc. Once the incoming activity passes a certain threshold a BOLD response becomes detectable by fMRI. A BOLD response can be quantified/described by the spatial distribution (small, large) or by parameters of the HRF (e.g. maximal BOLD signal intensity ($BOLD_{max}$), initial raising slope or the time between stimulus onset and maximal BOLD signal intensity (t_{max})). However, all these measurable parameters only reflect hemodynamic responses and the exact relations to the underlying changes in neuronal activities are still not known exactly. Previous combined electrophysiology fMRI studies indicate that the size of the BOLD response reflects rather the quality/quantity of local signal processing than specific forms of input, postsynaptic or output (spiking) activity.[10] Furthermore, recent studies demonstrated variable shapes of the HRF in different regions during one stimulus[37,38] or variable shapes of the HRF in one region during presentation of slightly different stimulations.[9] Therefore, the quality of local processing of incoming signals may also control the shape of the HRF.

In the present study, the two different perforant pathway stimulation protocols, i.e. continuous and discontinuous 100 Hz, triggered two HRFs in the mPFC/ACC that differed in the initial rising slope so that during continuous 100 Hz stimulations the $BOLD_{max}$ was reached 2 s later than during discontinuous 100 Hz stimulations (Figure 7(d)). Without concurrent measured electrophysiological signals this variation in the HRF cannot be linked to neurophysiological parameters of local signal processing. Nevertheless, the formation of BOLD responses depends on different forms of signal processing. During discontinuous 100 Hz stimulation significant BOLD responses were generated in the presence of MK801 or SCH23390, indicating that neither NMDA nor $D_{1/5}$ dopamine receptor-mediated processes were required. In contrast, during continuous 100 Hz stimulations both NMDA and $D_{1/5}$ dopamine receptor-mediated processes were required for the formation of BOLD responses in the mPFC/ACC. Thus, the shape of the HRF may give information about the signaling processes involved. However, it cannot serve as reference to one activated transmitter system, e.g. the dopaminergic system. Activation of dopamine receptors coincided with: (1) a delayed HRF during continuous 100 Hz pulse stimulation (Figure 7(d)), (2) no changes in the HRF when the VTA was optogenetically co-activated during discontinuous 100 Hz pulse stimulations and (3) an even faster initial raise during application of the dopaminergic agonist SKF83959 (Figure 5). Thus, the shape of the HRF is not controlled by dopamine itself but by how dopamine alters the local signal processing.

During continuous 100 Hz stimulation low pulse intensities (i.e. between 200 and 300 μA) were already sufficient to generate substantial BOLD responses outside the HC formation. Besides a pure summation effect, i.e. 100 pulses instead of 20 pulses, it is feasible that only the combination of glutamatergic projections from the VTA and hippocampus triggers BOLD responses in the mPFC/ACC. Since dopamine does not on its own modify the BOLD response, time-matched co-release of dopamine may optimize the interplay between individual glutamatergic inputs in such a way that the resultant local neuronal activity eventually affects BOLD signal intensities. There are some evidences for such a scenario. *First*, BOLD responses in the mPFC/ACC only depended on dopamine when the stimulation protocol induced an activation of the HC formation and VTA. *Second*, BOLD responses in the mPFC/ACC that were triggered by discontinuous 100 Hz pulses applied with similar low pulse intensities were not responsive to pharmacologically or optogenetically induced dopamine receptor activations. Consequently, dopamine release into the mPFC/ACC does not intrinsically modify local neuronal activity patterns in such a way that it becomes detectable by fMRI. *Third*, a previous experiment demonstrated that stimulation of the perforant pathway with discontinuous 100 Hz pulses caused BOLD responses in the mPFC/ACC that were significantly increased when the medial forebrain bundle, a fiber tract that includes glutamatergic and dopaminergic

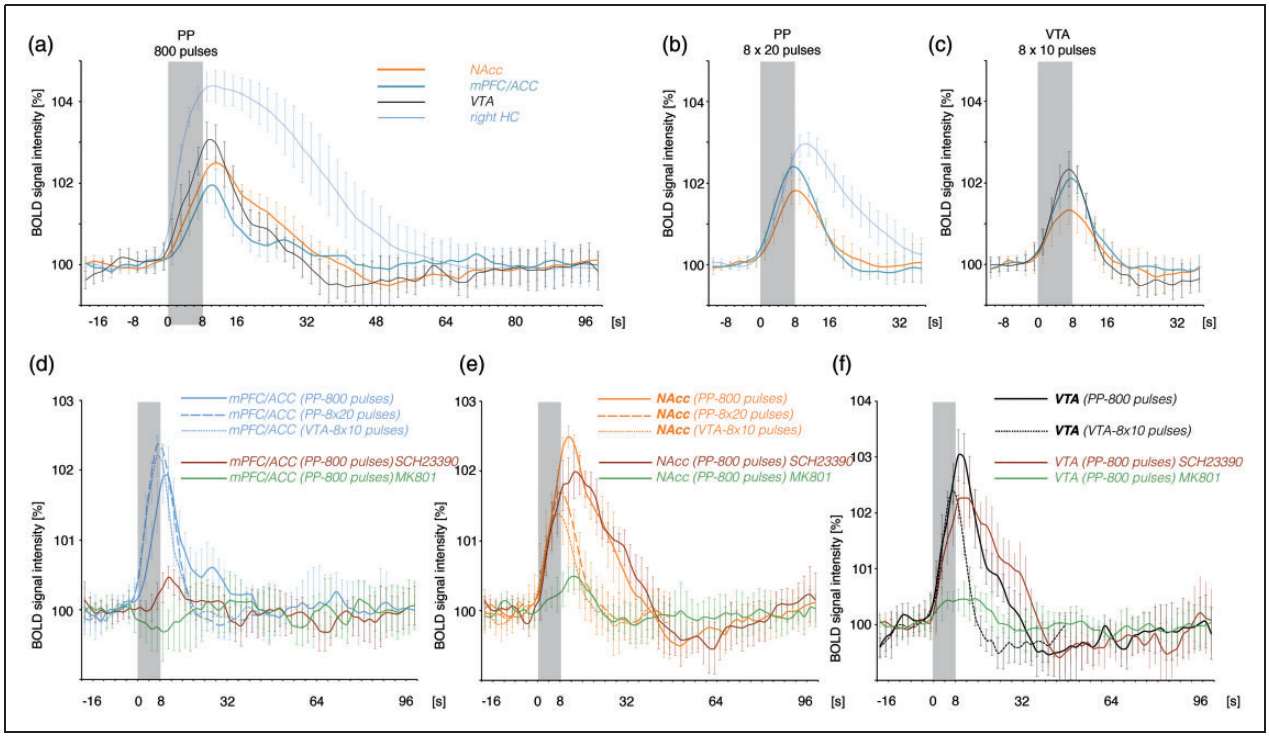

Figure 7. Summary of the observed BOLD responses during the applied stimulation protocols. The hemodynamic response functions (HRF), characterizing the BOLD response, are compared. (a) Electrical stimulation of the perforant pathway with continuous 100 Hz pulses for 8 s triggered BOLD responses in various regions of the rat brain. During this stimulation condition the maximal BOLD response in the NAcc (orange line) exceeded the maximal BOLD response in the mPFC/ACC (blue line). (b) Electrical stimulation of the perforant pathway with bursts of high-intensity pulses also triggered BOLD responses in various regions of the brain. Under this stimulation condition the BOLD response in the mPFC/ACC (blue line) exceeded the response in the NAcc (orange line). (c) Electrical stimulation of the VTA also triggered BOLD responses in various regions. Again the BOLD response in the mPFC/ACC (blue line) exceeded the response in the NAcc (orange line). (d) Comparison of the HRFs in the mPFC/ACC during all stimulation conditions. Whereas the initial slope of the HRF was similar during electrical VTA (dotted line) and high-intensity burst pulse stimulations of perforant pathway (dashed line), the initial slope was delayed during low-intensity continuously pulse stimulation (solid line). For comparison, the effects of SCH23390 (red solid line) and MK801 (green solid line) on the BOLD response during continuous 100 Hz pulse stimulations are included. (e) The initial slope of the HRF in the NAcc was similar during all stimulation conditions. The presence of MK801 almost abolished the formation of a BOLD response in the NAcc during continuous 100 Hz pulse stimulation. (f) The initial slope of the HRF observed in the VTA/SN region during electrical stimulation of the VTA (dotted line) and during electrical stimulation of perforant pathway with continuous 100 Hz pulses was identical. Again, the presence of MK801 inhibited the BOLD response in the VTA/SN region.
VTA: ventral tegmental area; mPFC/ACC: medial prefrontal/anterior cingulate cortex; NAcc: nucleus accumbens.

projections from the VTA, was electrically co-stimulated. Similarly, BOLD responses in the mPFC/ACC that were triggered by electrical medial forebrain bundle stimulation were increased when the HC formation was co-activated by discontinuous 100 Hz pulses.[38] These results imply that under conditions with complex inputs, e.g. from various regions, the dopaminergic system can control local signaling processes in such a way that they become detectable by fMRI.

In summary, our findings suggest that artificially induced dopamine release or pharmacological dopamine receptor activation is insufficient to elicit or modify the BOLD responses in the mPFC/ACC and NAcc. In specific contexts, however, mesolimbic dopamine can become a necessary component, permitting or modifying the formation of a BOLD response that is primarily driven by glutamatergic processes. These findings highlight the importance of a careful circuit-level analysis when BOLD responses are attributed to simultaneously released dopamine. The action of dopamine is highly complex and critically reliant on the underlying activity patterns of the circuits it acts on. Especially in human studies, in which invasive studies are mostly impossible, care must be taken not to assume falsely a simplified relationship of BOLD response and concurrent activation of the dopaminergic system.

Funding

The author(s) disclosed receipt of the following financial support for the research, authorship, and/or publication of this article: This work was supported by a grant from the Deutsche Forschungsgemeinschaft to F.A. (DFG An200-06).

Acknowledgments

We thank K. Krautwald and Silvia Vieweg for their excellent technical assistance.

Declaration of conflicting interests

The author(s) declared no potential conflicts of interest with respect to the research, authorship, and/or publication of this article.

Authors' contributions

MTL and FA contributed equally in the manuscript. CH performed electrical perforant pathway stimulation/MRI and fast-scan cyclic voltammetry experiments, MB performed optogenetic experiments, TS performed electrical VTA stimulation/fMRI experiments, MTL. design and performed optogenetic experiments and wrote the manuscript and FA designed and performed electrical perforant pathway stimulation/MRI and wrote the manuscript.

Supplementary material

Supplementary material for this paper can be found at http://jcbfm.sagepub.com/content/by/supplemental-data

References

1. Lisman JE and Grace AA. The hippocampal-VTA loop: controlling the entry of information into long-term memory. *Neuron* 2005; 46: 703–713.
2. Robinson DL, Heien ML and Wightman RM. Frequency of dopamine concentration transients increases in dorsal and ventral striatum of male rats during introduction of conspecifics. *J Neurosci* 2002; 22: 10477–10486.
3. Roitman MF, Stuber GD, Phillips PE, et al. Dopamine operates as a subsecond modulator of food seeking. *J Neurosci* 2004; 24: 1265–1271.
4. Schmidt HD, Famous KR and Pierce RC. The limbic circuitry underlying cocaine seeking encompasses the PPTg/LDT. *Eur J Neurosci* 2009; 30: 1358–1369.
5. Steinberg EE, Boivin JR, Saunders BT, et al. Positive reinforcement mediated by midbrain dopamine neurons requires D1 and D2 receptor activation in the nucleus accumbens. *PLoS One* 2014; 9: e94771.
6. Attwell D, Buchan AM, Charpak S, et al. Glial and neuronal control of brain blood flow. *Nature* 2010; 468: 232–243.
7. Attwell D and Iadecola C. The neural basis of functional brain imaging signals. *Trends Neurosci* 2002; 25: 621–625.
8. Heeger DJ and Ress D. What does fMRI tell us about neuronal activity? *Nat Rev Neurosci* 2002; 3: 142–151.
9. Angenstein F. The actual intrinsic excitability of granular cells determines the ruling neurovascular coupling mechanism in the rat dentate gyrus. *J Neurosci* 2014; 34: 8529–8545.
10. Angenstein F, Kammerer E and Scheich H. The BOLD response in the rat hippocampus depends rather on local processing of signals than on the input or output activity. A combined functional MRI and electrophysiological study. *J Neurosci* 2009; 29: 2428–2439.
11. Helbing C, Werner G and Angenstein F. Variations in the temporal pattern of perforant pathway stimulation control the activity in the mesolimbic pathway. *Neuroimage* 2013; 64C: 43–60.
12. Luo AH, Tahsili-Fahadan P, Wise RA, et al. Linking context with reward: a functional circuit from hippocampal CA3 to ventral tegmental area. *Science* 2011; 333: 353–357.
13. Choi JK, Chen YI, Hamel E, et al. Brain hemodynamic changes mediated by dopamine receptors: role of the cerebral microvasculature in dopamine-mediated neurovascular coupling. *Neuroimage* 2006; 30: 700–712.
14. Chen YC, Galpern WR, Brownell AL, et al. Detection of dopaminergic neurotransmitter activity using pharmacologic MRI: correlation with PET, microdialysis, and behavioral data. *Magn Reson Med* 1997; 38: 389–398.
15. Ren J, Xu H, Choi JK, et al. Dopaminergic response to graded dopamine concentration elicited by four amphetamine doses. *Synapse* 2009; 63: 764–772.
16. Schwarz AJ, Zocchi A, Reese T, et al. Concurrent pharmacological MRI and in situ microdialysis of cocaine reveal a complex relationship between the central hemodynamic response and local dopamine concentration. *Neuroimage* 2004; 23: 296–304.
17. Angenstein F, Krautwald K, Wetzel W, et al. Perforant pathway stimulation as a conditioned stimulus for active avoidance learning triggers BOLD responses in various target regions of the hippocampus: a combined fMRI and electrophysiological study. *Neuroimage* 2013; 75: 213–227.
18. Paxinos G and Watson C. *The rat brain in stereotaxic coordinates*. San Diego: Academic Press, 1988.
19. Hennig J, Nauerth A and Friedburg H. RARE imaging: a fast imaging method for clinical MR. *Magn Reson Med* 1986; 3: 823–833.
20. Kolodziej A, Lippert M, Angenstein F, et al. SPECT-imaging of activity-dependent changes in regional cerebral blood flow induced by electrical and optogenetic self-stimulation in mice. *Neuroimage* 2014; 103C: 171–180.
21. Yizhar O, Fenno LE, Prigge M, et al. Neocortical excitation/inhibition balance in information processing and social dysfunction. *Nature* 2011; 477: 171–178.
22. Fields HL, Hjelmstad GO, Margolis EB, et al. Ventral tegmental area neurons in learned appetitive behavior and positive reinforcement. *Ann Rev Neurosci* 2007; 30: 289–316.
23. Ohayon S, Grimaldi P, Schweers N, et al. Saccade modulation by optical and electrical stimulation in the macaque frontal eye field. *J Neurosci* 2013; 33: 16684–16697.
24. Liu XB and Jones EG. Localization of alpha type II calcium calmodulin-dependent protein kinase at glutamatergic but not gamma-aminobutyric acid (GABAergic) synapses in thalamus and cerebral cortex. *Proc Natl Acad Sci USA* 1996; 93: 7332–7336.

25. Koos T, Tecuapetla F and Tepper JM. Glutamatergic signaling by midbrain dopaminergic neurons: recent insights from optogenetic, molecular and behavioral studies. *Curr Opin Neurobiol* 2011; 21: 393–401.
26. Stuber GD, Hnasko TS, Britt JP, et al. Dopaminergic terminals in the nucleus accumbens but not the dorsal striatum corelease glutamate. *J Neurosci* 2010; 30: 8229–8233.
27. Sulzer D, Joyce MP, Lin L, et al. Dopamine neurons make glutamatergic synapses in vitro. *J Neurosci* 1998; 18: 4588–4602.
28. Tecuapetla F, Patel JC, Xenias H, et al. Glutamatergic signaling by mesolimbic dopamine neurons in the nucleus accumbens. *J Neurosci* 2010; 30: 7105–7110.
29. Margolis EB, Lock H, Hjelmstad GO, et al. The ventral tegmental area revisited: is there an electrophysiological marker for dopaminergic neurons? *J Physiol* 2006; 577(Pt 3): 907–924.
30. Swanson LW. The projections of the ventral tegmental area and adjacent regions: a combined fluorescent retrograde tracer and immunofluorescence study in the rat. *Brain Res Bull* 1982; 9: 321–353.
31. Hnasko TS, Hjelmstad GO, Fields HL, et al. Ventral tegmental area glutamate neurons: electrophysiological properties and projections. *J Neurosci* 2012; 32: 15076–15085.
32. Morales M and Root DH. Glutamate neurons within the midbrain dopamine regions. *Neuroscience* 2014; 282: 60–68.
33. Yamaguchi T, Wang HL, Li X, et al. Mesocorticolimbic glutamatergic pathway. *J Neurosci* 2011; 31: 8476–8490.
34. Carr DB and Sesack SR. GABA-containing neurons in the rat ventral tegmental area project to the prefrontal cortex. *Synapse* 2000; 38: 114–123.
35. Van Bockstaele EJ and Pickel VM. GABA-containing neurons in the ventral tegmental area project to the nucleus accumbens in rat brain. *Brain Res* 1995; 682: 215–221.
36. Ranck JB Jr. Which elements are excited in electrical stimulation of mammalian central nervous system: a review. *Brain Res* 1975; 98: 417–440.
37. Conner CR, Ellmore TM, Pieters TA, et al. Variability of the relationship between electrophysiology and BOLD-fMRI across cortical regions in humans. *J Neurosci* 2011; 31: 12855–13865.
38. Krautwald K, Min HK, Lee KH, et al. Synchronized electrical stimulation of the rat medial forebrain bundle and perforant pathway generates an additive BOLD response in the nucleus accumbens and prefrontal cortex. *Neuroimage* 2013; 77: 14–25.